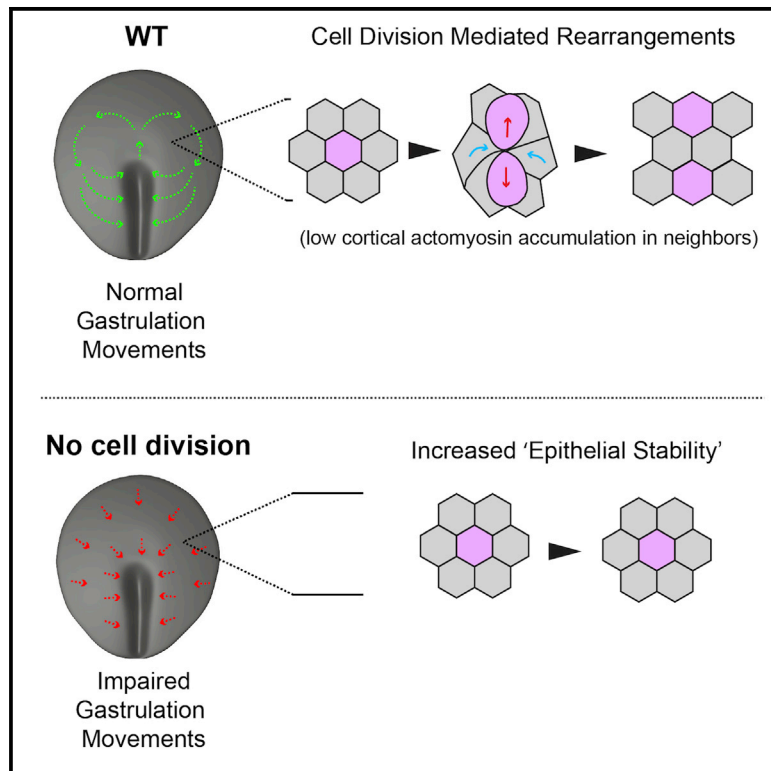# Cell Division Drives Epithelial Cell Rearrangements during Gastrulation in Chick

Graphical Abstract

Authors
Joao Firmino, Didier Rocancourt, Mehdi Saadaoui, Chloe Moreau, Jerome Gros

Correspondence
jgros@pasteur.fr

In Brief
Firmino et al. explore with live imaging how epithelial cells rearrange to shape complex tissues during amniote development. They show that during chick gastrulation, cell division powers dramatic epithelial cell rearrangements critical to the process. Low cortical actomyosin accumulation within epithelial cells enables dividing cells to remodel neighboring junctions.

Highlights

- Cell division is a major driver of epithelial cell rearrangement

- Cell division-mediated intercalations pattern gastrulation movements

- Epithelial cells exhibit low basolateral accumulation of cortical actomyosin

- Increasing cortical actomyosin accumulation in neighbors prevents rearrangements

Article

Cell Division Drives Epithelial Cell Rearrangements during Gastrulation in Chick

Joao Firmino,[1,2,4] Didier Rocancourt,[1,2,4] Mehdi Saadaoui,[1,2] Chloe Moreau,[1,2,3] and Jerome Gros[1,2,*]
[1]Department of Developmental and Stem Cell Biology, Institut Pasteur, 25 rue du Docteur Roux, 75724 Paris Cedex 15, France
[2]CNRS URA2578, rue du Dr Roux, 75015 Paris, France
[3]University Pierre et Marie Curie, Cellule Pasteur UPMC, rue du Dr Roux, 75015 Paris, France
[4]Co-first author
*Correspondence: jgros@pasteur.fr
http://dx.doi.org/10.1016/j.devcel.2016.01.007

SUMMARY

During early embryonic development, cells are organized as cohesive epithelial sheets that are continuously growing and remodeled without losing their integrity, giving rise to a wide array of tissue shapes. Here, using live imaging in chick embryo, we investigate how epithelial cells rearrange during gastrulation. We find that cell division is a major rearrangement driver that powers dramatic epithelial cell intercalation events. We show that these cell division-mediated intercalations, which represent the majority of epithelial rearrangements within the early embryo, are absolutely necessary for the spatial patterning of gastrulation movements. Furthermore, we demonstrate that these intercalation events result from overall low cortical actomyosin accumulation within the epithelial cells of the embryo, which enables dividing cells to remodel junctions in their vicinity. These findings uncover a role for cell division as coordinator of epithelial growth and remodeling that might underlie various developmental, homeostatic, or pathological processes in amniotes.

INTRODUCTION

During embryonic development, gastrulation is the first major morphogenetic event that leads to the formation of the three embryonic layers (i.e. ectoderm, mesoderm, and endoderm). In chick, gastrulation involves large-scale cellular movements, taking place within the single-celled layer epithelial embryo. These cell movements, first described in 1929 (Gräper, 1929; Wetzel, 1929), were named "Polonaise movements" due to their resemblance to a Polish dance choreography: upon incubation, within the flat epiblast disk, two counter-rotational flows of cells merge at the posterior end of the embryonic disk to form the primitive streak (i.e. the site of mesendoderm formation and future midline of the embryo). More recently, it has been shown that the primitive streak progressively forms and elongates through cell shape changes, mediolateral intercalation, and ingression of epithelial cells at the posterior margin of the epiblast (Rozbicki et al., 2015; Voiculescu et al., 2007, 2014). Although such cell-cell

interactions have been elegantly demonstrated to drive streak elongation, they do not provide, on their own, a plausible explanation for the circular flows of cells concomitantly observed in the epiblast. In their models, Voiculescu et al. and Rozbicki et al. propose that the cell displacements induced by shape changes, ingressions, and intercalations at the streak are "propagated" throughout the epiblast. These peculiar cell movements taking place in the epithelial embryo, where cells are connected by adherens junctions, pose a conceptual problem: How can movements be propagated within the rapidly growing epiblast without disrupting the epithelial integrity of the embryo? Do cells rearrange within the epiblast or exhibit specific behaviors participating in the spatial patterning of gastrulation movements? If so, what are the underlying cellular and molecular mechanisms?

Epithelial rearrangement events have been extensively characterized in invertebrates, particularly *Drosophila*. In this model, a number of stereotyped key events (for review see Guillot and Lecuit, 2013a), have been identified. During germband elongation in *Drosophila*, an ordered process of cell intercalation such as T1 processes (involving four cells) (Bertet et al., 2004), and the formation/resolution of rosettes (involving five cells or more) (Blankenship et al., 2006) underlies the elongation of the embryo: epithelial cells undergo planar polarized remodeling of junctions driven by a myosin-dependent junction shortening in one plane, followed by lengthening in the perpendicular plane. Epithelial cells have also been shown to rearrange through T2 processes, during which junctions are removed by a cell extrusion mechanism, as observed in the *Drosophila* notum (Marinari et al., 2012).

During all the aforementioned processes, cells do not divide. The process of cell division has been shown to play important roles in epithelial tissue morphogenesis in zebrafish and *Drosophila*, in particular through polarized orientation, which can be instructed by signaling pathways (Baena-López et al., 2005; Gong et al., 2004; Saburi et al., 2008; for review see Morin and Bellaïche, 2011) or in response to mechanical stress (Campinho et al., 2013; LeGoff et al., 2013; Mao et al., 2013; Wyatt et al., 2015). However, cell division itself does not directly promote rearrangements of epithelial cells: upon cell division, it has been reported that daughter cells almost always share a common interface and do not intercalate between their neighbors (Bischoff and Cseresnyés, 2009; Gibson et al., 2006). Aside from the addition of a novel cell-cell junction at the interface between the two daughters, the overall junctional organization and, therefore, the epithelial topology remain globally unchanged. This is exemplified by numerous clonal analyses performed in *Drosophila* whereby

clonal descendants remain compact and do not disperse within the epithelial tissue (Knox and Brown, 2002). Recently, the mechanisms underlying the formation of a new daughter-daughter cell junction have been brought to light. Studies performed in the *Drosophila* early embryonic and pupal notum epithelia have shown that cell division can be regarded as a multicellular process involving not only a dividing cell but also its immediate neighbors. These studies show that as cytokinesis takes place, the contractile tension exerted by the cytokinetic ring of a dividing cell is resisted by its neighbors (actomyosin-based cortical tension). This ratio of forces at the site of cytokinesis ultimately results in local adhesion disengagement of the dividing cell with its neighbor, the annealing of the two daughter membranes, and the subsequent formation of a new daughter-daughter cell junction (Founounou et al., 2013; Guillot and Lecuit, 2013a; Herszterg et al., 2013). The observation that cell division does not directly promote epithelial cell rearrangements does not appear to be confined to *Drosophila* epithelia but can also be observed in the developing epithelia of *Caenorhabditis elegans*, zebrafish, and *Xenopus* (Harrell and Goldstein, 2011; Kieserman et al., 2008; Olivier et al., 2010), and has been implied to be a conserved feature among Metazoa (Gibson et al., 2006). Recently, cell division has been observed to be associated with cell dispersal in the mouse ureteric bud (Packard et al., 2013) and with rearrangements during mouse limb ectoderm morphogenesis (Lau et al., 2015). These studies have observed that in mouse, daughter cells do not necessarily share a common interface, questioning the universality of a daughter-daughter cell junction formation upon epithelial cell division in Metazoa. However, these studies did not examine the role of cell division in cell-cell intercalations and in overall epithelial morphogenesis. It thus remains unaddressed whether cell division acts as a regulatory mechanism in epithelial rearrangements and in epithelial morphogenesis in general, or whether these rearrangements associated with cell division are only incidental. Importantly, these observations beg the question of the underlying molecular mechanisms that would allow dividing cells to promote rearrangements, as opposed to what has been observed in epithelia of *Drosophila*, *C. elegans*, zebrafish, and *Xenopus*.

Here, we investigate the cellular mechanisms underlying the spatial patterning of gastrulation movements in chick and the role of cell division in this process. The early chick embryo develops as a flat, highly proliferative epithelial disk that can be easily live-imaged for long periods of time; it is thus an excellent system to study dynamic epithelial rearrangements in an amniote system. Using this model, we find that cell division promotes dramatic rearrangements of epithelial cells, and show that these rearrangements play a critical role in the spatial patterning of gastrulation movements; furthermore, we bring evidence that cell-cell intercalations induced by division are the consequence of an interplay between the actomyosin cytoskeleton of dividing cells and the cortical actomyosin of their immediate neighbors, which enables dividing cells to remodel junctions in their vicinity.

RESULTS

Cell Division Is a Major Epithelial Rearrangement Driver during Gastrulation

Previous studies focused on the cellular events driving primitive streak formation. Here, we decided to investigate whether cells of the epiblast away from the presumptive primitive streak, which actually display the rotational movements, exhibit specific behaviors that could play a role in the spatial patterning of these characteristic movements. To visualize gastrulation movements as they are taking place, we electroporated stage X chick embryos (Eyal Giladi-Kochav staging system, 0 hr of incubation) with a GFP reporter gene and followed the behavior of electroporated cells at stage 3 (Hamburger and Hamilton staging system, around 12–15 hr of incubation) using the EC culture system (Chapman et al., 2001) and confocal microscopy (10× objective, Figure 1A and Movie S1). Using high-resolution (40× objective) confocal microscopy, we unexpectedly observed that at around stage 3, as gastrulation movements are taking place, most daughter cells rapidly separate from each other in regions away from the primitive streak (Figure 1B and Movie S1). This observation is in sharp contrast to what has been previously observed in other epithelia (e.g. in *Drosophila*, *C. elegans*, zebrafish, and *Xenopus* embryos), where daughter cells almost always remain in contact (Bischoff and Cseresnyés, 2009; Campinho et al., 2013; Gibson et al., 2006; Harrell and Goldstein, 2011; Kieserman et al., 2008). Since epiblast cells are connected by adherens junctions of E-cadherin, we reasoned that neighboring cells must intercalate in between daughter cells to maintain epithelial integrity. To verify this, we live-imaged transgenic chicken embryos expressing a membrane-bound GFP (memGFP) (Rozbicki et al., 2015) to reveal all cell boundaries within the epiblast from stage X until stage 3+. Large epithelial regions (approximately 5,000–10,000 cells, 1 mm^2), anterior and lateral to the primitive streak-forming region (at approximately 500 μm distance), were imaged and analyzed (see Figure 1C and Movie S2). Interestingly, we found that at stage X, following cell division, most daughter cells remain in direct contact for at least 30 min after cytokinesis has been completed (90%, n = 738, 7 embryos; Figures 1D and 1E, and Movie S2). However, as gastrulation movements take place, epithelial cells in contact with a mitotic cell increasingly intercalate in between daughter cells (within 30 min after cytokinesis has completed), reaching 90% of intercalations at stage 3 (n = 530, 5 embryos; referred to as cytokinesis-mediated intercalation [CMI]; Figures 1D, 1F, 1G, and Movies S1 and S2). In addition to neighboring cells intercalating in between daughter cells, we noticed that daughter cells themselves also intercalate in between their neighbors (referred as daughter cell-associated intercalation [DCAI]; Figure 1F, and Movies S1 and S2). Notably, as observed for CMI, most division events promoted DCAI (93%).

We next sought to quantify the proportion of cell division-mediated intercalations (including both CMI and DCAI) in relation to other epithelial cell rearrangement events. This was done by analyzing the evolution of every junction within a given region of memGFP transgenic embryos, over a 1-hr period at stage 3, as gastrulation movements are taking place (n = 1,150 junctions analyzed, 5 embryos; for explanation of how junction states were assigned, see Experimental Procedures and Movie S3). We found that 63% of cell-cell junctions did not remodel (i.e. did not undergo any transitions; referred to as "stable"); only 13% of junctions remodeled without involving cell division (i.e. T1 or T2 processes; referred to as "T processes"), whereas 24% of junctions remodeled involving a cell division event (cytokinesis-mediated transitions 11%, and daughter cell-associated
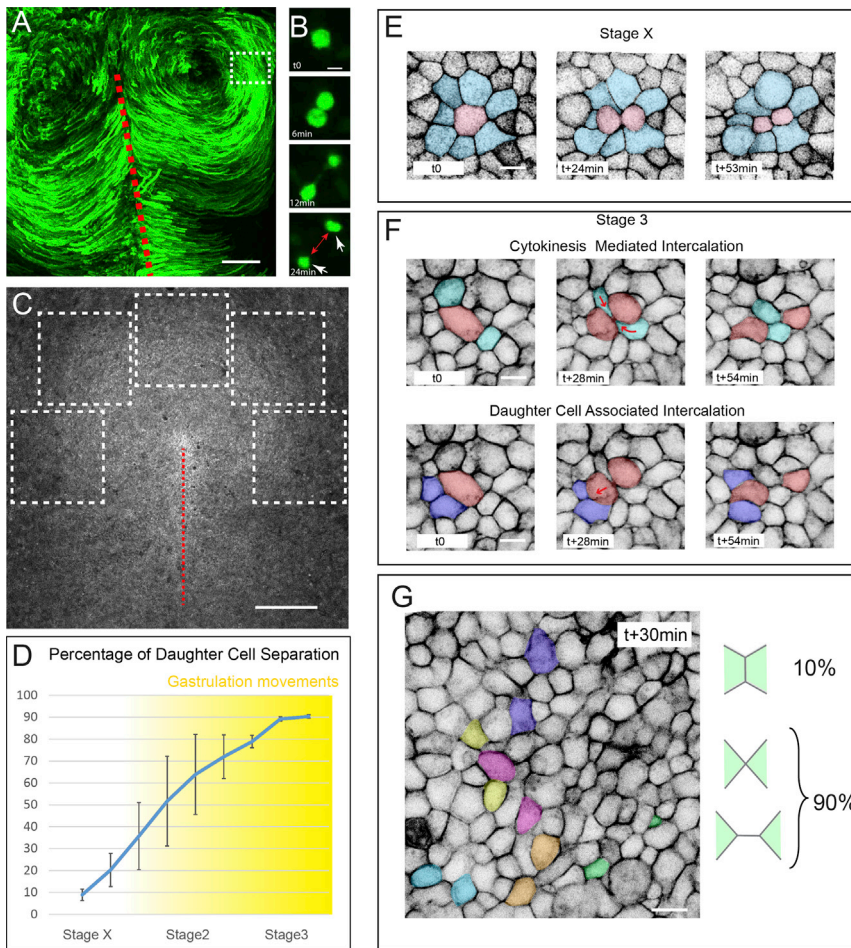
Figure 1. Cell Division Drives Epithelial Cell Intercalation

(A) Maximum projection of time series from a 3-hr time-lapse experiment of a chick embryo electroporated with a GFP reporter gene, showing the counter-rotational movements of epiblast cells at stage 3+. The primitive streak is indicated by a red dotted line.

(B) Time series in a region away from the primitive streak equivalent to the boxed region in (A) showing that upon cell division, daughter cells (white arrows) separate away from each other (red arrows).

(C) Dorsal view of a stage 3 memGFP transgenic chicken embryo acquired at 10× with the tiling/stitching module of the confocal microscope. The dotted white boxes depict the regions analyzed in (D); the primitive streak is indicated by a red dotted line.

(D) Percentage of daughter cell separation following cell division between stage X and 3+. Cell separation was scored every 2 hr; n = 2,997; 7 embryos. Error bars represent SEM.

(E and F) Time series of a stage X (E) and stage 3 (F) memGFP transgenic chick embryo highlighting the fate of a dividing cell (in red) and its immediate neighbors (in blue). At stage X (E), daughter cells do not rearrange.

(G) Image of a memGFP transgenic chick embryo from a time-lapse experiment highlighting daughter cells (colored cells) that have rearranged within 30 min after cell division.

Scale bar represents 200 μm in (A), 500 μm in (C), and 10 μm in (B), (E), (F) and (G). See also Movies S1 and S2.

---

transitions 13%; Figures 2D, 2D′, 2F, and Movie S3). Thus, cell division-mediated intercalations account for the vast majority of junctional remodeling events occurring in the highly proliferating epiblast, away from the primitive streak and as gastrulation movements take place.

Cell Division-Mediated Intercalations Are Necessary for the Spatial Patterning of Gastrulation Movements

We next investigated the potential role of cell division-mediated intercalations in contributing to the spatial patterning of gastrulation movements. Previous studies have shown that inhibition of cell division strongly affects cell movements during chick gastrulation, a phenotype attributed to a failure of the embryonic tissue to expand through an increase in cell number (Cui et al., 2005). In light of our findings, we decided to re-investigate the effect of the inhibition of cell division on the gastrulation movements and, importantly, on cell rearrangements. In control GFP electroporated embryos, the two counter-rotational flows of cells continuously take place (Figures 2A–2C and 2A′–2C′; Movie S1). However, upon aphidicolin exposure, a potent DNA polymerase inhibitor that indirectly prevents cell division uniformly within the epithelial embryo, movements still occurred but the typical circular pattern was rapidly impaired. At the concentration we used, aphidicolin induced an 80% decrease in cell divi-

sion compared with control embryos (as counted per number of dividing cells/μm^2 per hour, n = 2,140 cells, 4 embryos; see Experimental Procedures for details). Importantly, cells did not display symmetrical rotational movements but instead converged toward the primitive streak (Figures 2G–2I and 2G′–2I′; Movie S4), confirming previous observations (Cui et al., 2005). These results suggest that cell division does not act as a driving force of gastrulation movements but rather appears to be important for their spatial patterning. We therefore analyzed cell-cell junctions over time in aphidicolin-treated memGFP transgenic embryos to gain insights into the cell rearrangements taking place when cell division is abrogated. Not surprisingly, in this condition cell division-mediated intercalation events were almost completely abrogated (1%) (Figures 2J, 2J′, and 2F; Movie S3). Importantly, 89% of epithelial junctions were stable while only 10% of junctions exhibited cell division-independent rearrangements (T processes) (n = 832 junctions, 4 embryos). Thus, inhibition of cell division "stabilized" epithelial organization over time, which resulted in few cell rearrangements compared with control embryos (Figures 2E, 2E′, 2K, and 2K′; Movie S3). Of note, very similar results were obtained using aminopterin, a different compound causing cell division inhibition (89% decrease in cell division, as counted per number of dividing cells/μm^2 per hour; n = 1,500 cells, 3 embryos) through
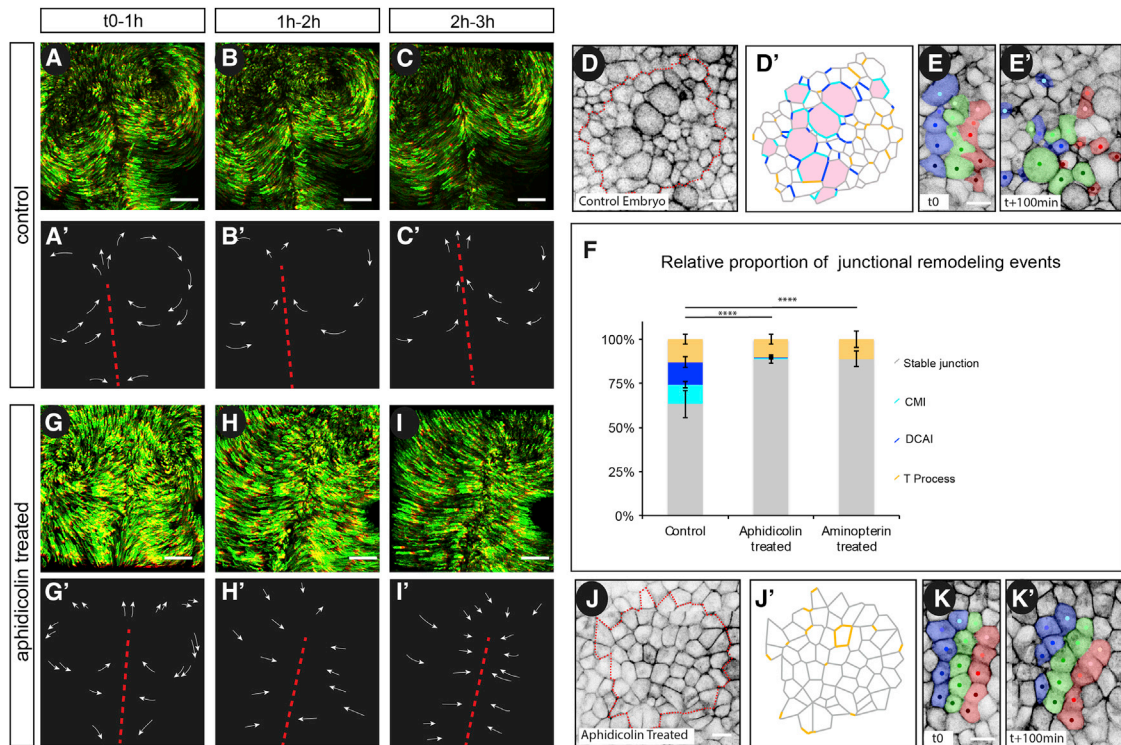
Figure 2. Cell Division Events and Their Associated Rearrangements Are Necessary for the Spatial Patterning of Gastrulation Movements

(A–C) Maximum projection of time series from a time-lapse experiment of a wild-type GFP electroporated embryo. The last ten time points have been pseudo-colored in red. (A′–C′) Cartoon depicting the trajectories of a few cells, the position of the primitive streak is indicated by a red dotted line.

(D) First time point of a 1-hr time-lapse experiment of a memGFP wild-type embryo, showing the region used for junction transition analyses in (D′). (D′) Cartoon schematizing transitions that each cell-cell junction will undergo over 1 hr in the region boxed in (D). "Stable" junctions, CMI transitions, DCAI, transitions, and "T" transitions are shown in gray, light blue, dark blue, and orange, respectively (see Experimental Procedures and Movie S3, for explanation on junction state assignment); cells that will divide are colored in red.

(E) Time series of a wild-type memGFP embryo on which stripes of cells and their progeny have been artificially labeled (in blue, green, and red) to reveal changes in cell organization between t0 (E) and t + 100 min (E′). Note that in wild-type embryos the cells disperse widely.

(F) Quantifications of the relative proportion of Stable, CMI, DCAI, and T-process transitions in wild-type, aphidicolin-treated, and aminopterin-treated embryos. Error bars represent SEM.

(G–I) Maximum projection of time series from a time-lapse experiment of an aphidicolin-treated and GFP electroporated embryo. Color scheme as in (A)–(C). (G′–I′) Cartoon depicting the trajectories of a few cells. Color scheme as in (A′)–(C′).

(J) First time point of a 1-hr time-lapse experiment of a memGFP aphidicolin-treated embryo, showing the region used for junction transition analyses in (J′). (J′) Cartoon schematizing transitions that each cell-cell junction will undergo over 1 hr in the region boxed in (J). The same color code used in (D) is applied.

(K) Time series of an aphidicolin-treated memGFP embryo on which stripes of cells and their progeny have been artificially labeled (in blue, green, and red) to reveal changes in cell organization between t0 (K) and t + 100 min (K′). Note that the cellular organization remains almost unchanged.

Error bars represent SEM with χ^2 test p value between bars, ****p < 0.0001. Scale bar represents 200 μm in (A)–(C) and (G)–(I), and 10 μm in (D)–(E) and (J)–(K). See also Figure S1, and Movies S3 and S4.

thymidylate depletion (Figures 2F and S1). Taken together, these data demonstrate that cell division acts as a powerful and major epithelial cell remodeling driver that enables the continuous cell rearrangements necessary to spatially pattern movements during gastrulation.

Cell Division Actively Promotes Epithelial Rearrangements

It has recently been described that primitive streak formation that is driven by cell intercalation and ingression is accompanied by the appearance of local directed strains within the epiblast (Rozbicki et al., 2015). Because in other systems directed strains have been shown to orient cell division to relieve tension within epithelial tissue (Campinho et al., 2013; LeGoff et al., 2013;

Mao et al., 2013; Wyatt et al., 2015), we sought to determine whether daughter cell separation could also be a tension-relieving mechanism and, therefore, a passive consequence of external forces arising from the primitive streak-forming region. First, we determined the timing of daughter cell separation relative to initiation of gastrulation movements. We found that the onset of daughter cell separation preceded by a few hours the appearance of local movements within the epiblast (Figure 1D). Therefore it is very unlikely that local directed strains induced by the primitive streak-forming region could account for the initiation of daughter cell separation. Second, if daughter cell separation is a consequence of external forces at work within the epiblast, then orientation of cell division (and subsequent intercalations) should be aligned with local tissue movements, as
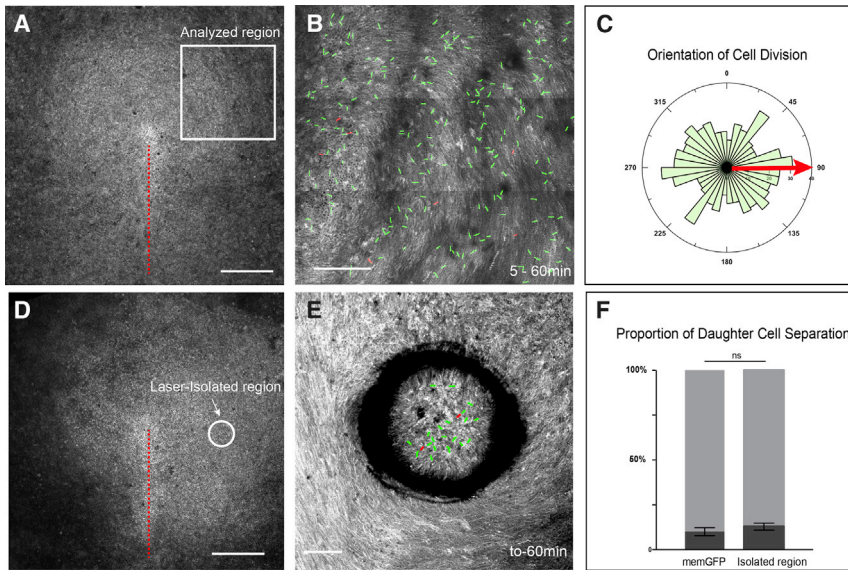
Figure 3. Cell Division Actively Promotes Epithelial Rearrangements

(A) Dorsal view of a stage 3 memGFP transgenic chicken embryo acquired at 10× with the tiling/stitching module of the confocal microscope. The white box depicts the location of regions analyzed, as shown in (B); the primitive streak is indicated by a red dotted line.

(B) Maximum-intensity projection of time points of a 1-hr time-lapse experiment in a region lateral to the primitive streak as shown in (A). Red lines point at cell divisions that lead to daughter cell juxtaposition, and green lines to daughter cells that separate from each other. Projection of the memGFP signal allows the visualization of the global tissue movement.

(C) Quantification of cell division orientation normalized to local tissue movement (red arrow). Note that no specific alignment of cell division with tissue flow can be observed (χ^2 test, p = 0.85).

(D) Dorsal view of a stage 3 memGFP transgenic chicken embryo acquired at 10× with the tiling/stitching module of the confocal microscope. The white circle depicts a region that was laser isolated; the primitive streak is indicated by a red dotted line.

(E) Maximum-intensity projection of time points of a 1-hr time-lapse experiment of the laser-isolated region shown in (D). Red lines point at cell divisions that lead to daughter cell juxtaposition, green lines to daughter cells that separate from each other. Projection of the memGFP signal allows visualization of the global tissue movement. Note that tissue flow is normal outside of the isolated region but abrogated in the isolated region.

(F) Quantifications of the proportion of daughter cell separation in control and laser-isolated epithelial regions (light gray: separated daughter cells; dark gray: daughter cells in contact). Two-way ANOVA test showed no significant difference (ns). Error bars represent SEM

Scale bar represents 500 μm in (A) and (D), 200 μm in (B), and 100 μm in (E). See also Movie S5.

observed in other systems (Campinho et al., 2013; LeGoff et al., 2013; Mao et al., 2013; Wyatt et al., 2015). We therefore quantified the orientation of cell division in regions of the epiblast away from the primitive streak-forming region and normalized the angles of cell division with respect to the local tissue flow. We could not find any sign of alignment of cell division orientation with the local tissue flow, which appeared largely isotropic (Figures 3A–3C and Movie S2; n = 390 cells, 3 embryos, χ^2 test p = 0.85), further supporting that external forces do not act to promote daughter cell separation. Finally, to functionally address whether external forces act to separate daughter cells upon division, we used UV laser microdissection in stage 3 embryos to isolate epithelial regions of the epiblast, thereby alleviating these regions from primitive streak-induced external forces. Laser microdissection efficiently resulted in isolation of epithelial regions (about 1,000 cells) from the rest of the embryo, which were then analyzed for 1 hr using live imaging microscopy (Figures 3D and 3E; Movie S5). Whereas tissue flow was close to normal outside the isolated regions (i.e. cells displayed rotational movement), tissue flow within isolated regions was abrogated, demonstrating that such isolated regions behave independently of the rest of the embryo and, therefore, independently of local directed strains arising from the primitive streak-forming region. Importantly, in these isolated regions the proportion of daughter cell separation showed no significant differences compared with stage 3 control embryos (Figure 3F; n = 182, 4 embryos). Altogether, these results demonstrate that cell division-mediated rearrangements arise from an active process and are not the consequence of external mechanical stimuli. Moreover, these results suggest that such cell behavior is an inherent property of the epithelial embryonic tissue at this stage.

Spatiotemporal Characterization of Cell Division-Mediated Intercalations

Next, we investigated how cell division-mediated intercalations are spatiotemporally controlled. Because cell division promotes cellular rearrangements at stage 3 but not at stage X, comparison between these stages can provide clues for mechanisms underlying cell division-mediated intercalations. We used high-resolution 4D (x, y, z, t), two-photon live imaging microscopy on memGFP transgenic embryos to capture a dividing cell and its neighbors in both space and time. At stage 3, we observed that cell division-mediated intercalation is a multistep process: First, as the dividing cell rounds up apically, neighboring cells become dramatically deformed and concomitantly establish novel contacts basally. Second, as the cytokinetic ring contracts from basal to apical, the contact between the dividing cell and its neighbors is carried along; Third, this novel cell contact finally expands into a stable cell-cell junction in the plane of the epithelium (Figures S2A, S2A′, and S2A″). In contrast, at stage X, as cells round up and start dividing, neighbors undergo only very local deformations and stable contacts between originally distant neighbors is not observed basally; instead a daughter-daughter cell junction forms almost immediately (Figures S2B, S2B′, and S2B″). Furthermore, analysis of junctions at stage X revealed that the epithelium is very "stable" (92%) with few T processes, CMI, and DCAI (5%, 2%, and 1%, respectively; n = 551, 2 embryos) (Figure S2C). These observations suggest that at stage 3 the dividing cells are able to dramatically deform and displace neighbors, eventually bringing them into contact between daughter cells, whereas at stage X cells divide in a highly stable epithelium that might prevent dividing cells from rearranging junctions in their vicinity.
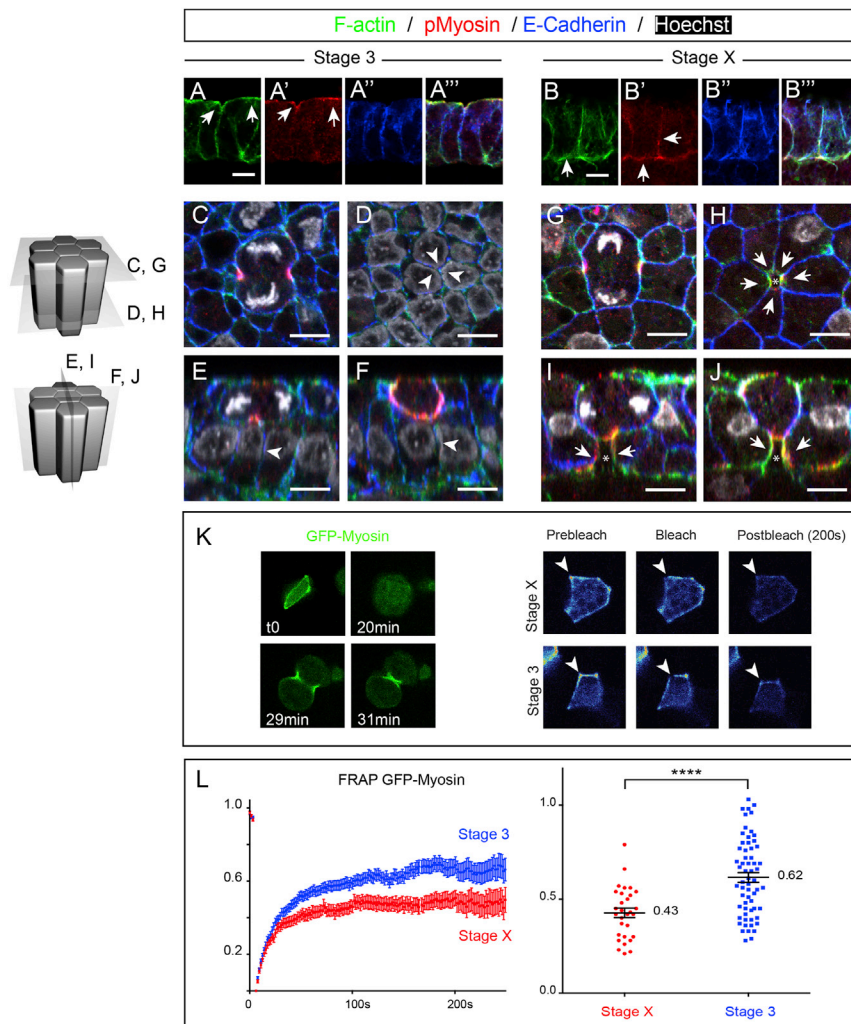
F-actin / pMyosin / E-Cadherin / Hoechst

Figure 4. E-Cadherin, F-Actin, and pMyosin Localization and Myosin Dynamics before and during Gastrulation Movements

(A and B) Transverse cryosections of stage 3 (A) and stage X (B) embryos stained with phalloidin (A and B), pMyosin (A′ and B′), and E-cadherin (A″ and B″) antibodies. (A‴) and (B‴) show the merged pictures. Arrows point to F-Actin and pMyosin accumulation.

(C–J) Confocal ortho-slices of stage 3 (C–F) and stage X (G–J) whole-mount embryos stained with phalloidin, pMyosin, and E-cadherin antibodies. Arrows indicate F-actin and pMyosin accumulation, asterisks show free-contact cell interfaces, and arrowheads indicate basal E-cadherin junctions.

(K) Left panel: Time series of a GFP-Myosin electroporated cell showing localization at the cortex and the cytokinetic furrow in a stage 3 embryo. Right panel: Example of images used for GFP-Myosin (heatmap color code) FRAP experiments, showing the region used for FRAP (arrowhead) of epithelial cells in stage X and stage 3 embryos.

(L) Left panel: FRAP curves of cortical GFP-Myosin in stage X (red) and stage 3 (blue) embryos. Errors bars indicate SEM; n = 30 and n = 61 for stage X and stage 3, respectively. Right panel: Common plot of mobile fraction for all FRAP experiments done at stages X and 3; associated average numbers of the mobile fraction of each fitted curve and statistical significance between the two stages were obtained by a Mann-Whitney test, ****p < 10^{-5}.

Scale bar represents 10 μm. See also Figures S2–S4.

Differences in F-Actin and Myosin Localization and Dynamics Underlie Cell Division-Mediated Rearrangements

For dividing cells to mechanically deform neighbors and displace them, we reasoned that non-dividing epithelial cells must exhibit relatively low cortical rigidity (allowing neighbor deformation) as well as low cell-cell junction stability (allowing planar displacement through junction exchange). Because, at the molecular level, both low cortical rigidity and low E-cadherin junction stability have been linked to high actomyosin cytoskeleton turnover (Sheikh et al., 1997; Cavey and Lecuit, 2009; Cavey et al., 2008; Engl et al., 2014; Wu et al., 2014), we decided to first check for differences in E-cadherin, F-actin, and phosphorylated myosin II (pMyosin) protein localization between stage X and stage 3 epithelia, in dividing cells and their neighbors.

Immunofluorescence on transverse sections at stage 3 showed that E-cadherin in chick epiblast cells was distributed along the entire apico-basolateral extent of non-dividing epithelial cells; F-actin localized also along the apico-basolateral cortex of epithelial cells, whereas pMyosin was predominantly enriched apically (Figures 4A–4A‴; see also Figure S4 for quantifications of fluorescence intensity profile). Whole-mount stain-

ings on fixed embryos showed that, as observed in 4D live imaging experiments, when cells enter division a long E-cadherin-positive cell interface between seemingly distant neighbors (as observed apically) can already be seen basally (Figures 4C–4F, white arrowheads; see also Figures S3A–S3L; n = 11 out of 11 cells, 3 embryos). In contrast, examination at stage X, when cell division does not promote epithelial cell intercalation, revealed interesting differences. Whereas E-cadherin was also found along the whole basolateral extent of epithelial cells, pMyosin and F-actin showed greater accumulation along the basolateral cortex of epithelial cells (Figures 4B–4B‴, white arrowheads; see also Figure S4 for quantifications of fluorescence intensity profile). Whole-mount stainings on fixed specimens showed that as cells entered division, neighboring cells in contact with the dividing cell exhibited a dramatic accumulation of actin and myosin specifically at the basolateral side (Figures 4G–4J, white arrows; see also Figures S3M–S3X; n = 9 out of 10 cells, 3 embryos). This accumulation of actin and myosin in neighbors seemed to prevent the formation of a stable basolateral contact between distant neighbors (as observed in stage 3 embryos) since contact-free cell interfaces (devoid of E-cadherin staining) could be concomitantly observed directly beneath the dividing cells (white arrows and asterisks in Figures 4H–4J; see also Figures S3M–S3X). Such observations are reminiscent of the
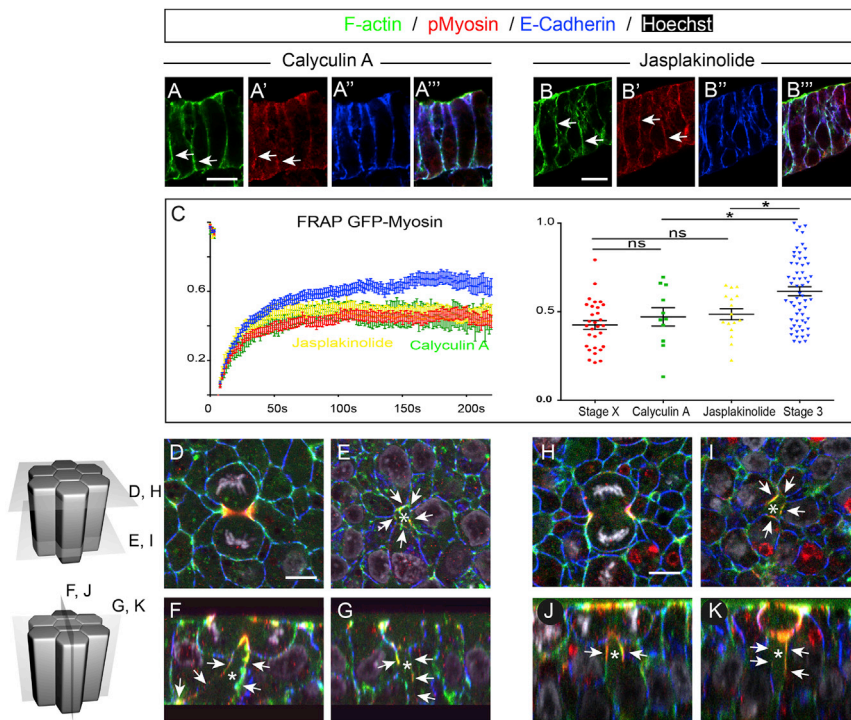
mechanisms observed in epithelial cells of the *Drosophila* notum (Fouununou et al., 2013; Herszterg et al., 2013), and adhesion disengagement in the *Drosophila* embryo (Guillot and Lecuit, 2013b) during the generation of a daughter-daughter cell interface, although in chick myosin accumulation and adhesion disengagement of the dividing cell with its neighbor does not take place apically but basolaterally.

We furthermore checked whether differences in actomyosin dynamics between these two stages might underlie cell division-mediated rearrangements. We used fluorescence recovery after photobleaching (FRAP) to quantitatively measure Myosin dynamics at the cortex of epithelial cells at stage 3, when cells exhibit cell division-mediated rearrangements, and at stage X, when cells do not undergo cell division-mediated intercalations, and checked for notable differences. To this end, we electroporated a GFP protein fused to the chicken myosin light chain 2 protein (GFP-Myosin), which localized predominantly to the cell cortex and to the actomyosin ring as cells divided (Figure 4K, left panel). GFP-Myosin did not interfere with cell division nor normal embryonic development after 24 hr (data not shown), strongly arguing that the GFP-Myosin fusion protein does not interfere with endogenous myosin and that it can be used to monitor its dynamics. By performing FRAP on cortical GFP-Myosin of randomly chosen non-dividing cells (Figure 4K, right panel), we found that GFP-Myosin dynamics were different between stage X and stage 3. At stage X, when cells do not undergo cell division-mediated intercalations, the mobile fraction was much lower (43%, n = 30) than in epithelial cells of stage 3 embryos (62%, n = 61) (Figure 4L). Thus, these results show that myosin stability at the cortex is significantly lower in epithelial cells of stage 3 embryos compared with stage X. Altogether, these results show that differences in cortical actin and pMyosin

localized accumulation, and at least in myosin dynamics, underlie cell division-mediated rearrangements.

Increasing F-Actin and Myosin Stability Impairs Cell Division-Mediated Rearrangements

We finally functionally tested whether such observed differences in actomyosin cytoskeleton between stages X and 3 might regulate cell division-mediated intercalations. To this end we took advantage of two compounds, the F-actin stabilizing peptide jasplakinolide (Bubb et al., 1994), and the myosin II phosphatase inhibitor calyculin A (Ishihara et al., 1989), which allowed us to uniformly increase actomyosin stability in all epithelial cells of stage 3 embryos. Both compounds induced F-actin and myosin enrichment at the cortex of epithelial cells as shown on transverse sections (Figures 5A–5A‴ and 5B–5B‴, white arrows; see also Figure S4 for quantifications of fluorescence intensity profile) and whole-mount embryos (Figures S5A–S5I). Moreover, FRAP experiments on GFP-Myosin electroporated embryos at stage 3 showed that in the presence of jasplakinolide and calyculin A, the mobile fraction was much lower (49%, n = 16 and 47%, n = 11, respectively) than in stage 3 control embryos (Figure 5C). These results confirmed that in these drug-treated embryos myosin stability at the cortex was dramatically increased, resembling dynamics observed in stage X embryos. Notably, we noted an increased co-localization of F-actin with E-cadherin at cell junctions, in agreement with higher junction stability (Figure S6). We next examined the localization of these proteins in dividing cells and their immediate neighbors (Figures 5D–5K). We found that as cells divided in embryos treated with calyculin A or jasplakinolide, a dramatic accumulation of pMyosin and F-actin in neighbors was found along the basolateral extent of neighbors, directly beneath the dividing cells
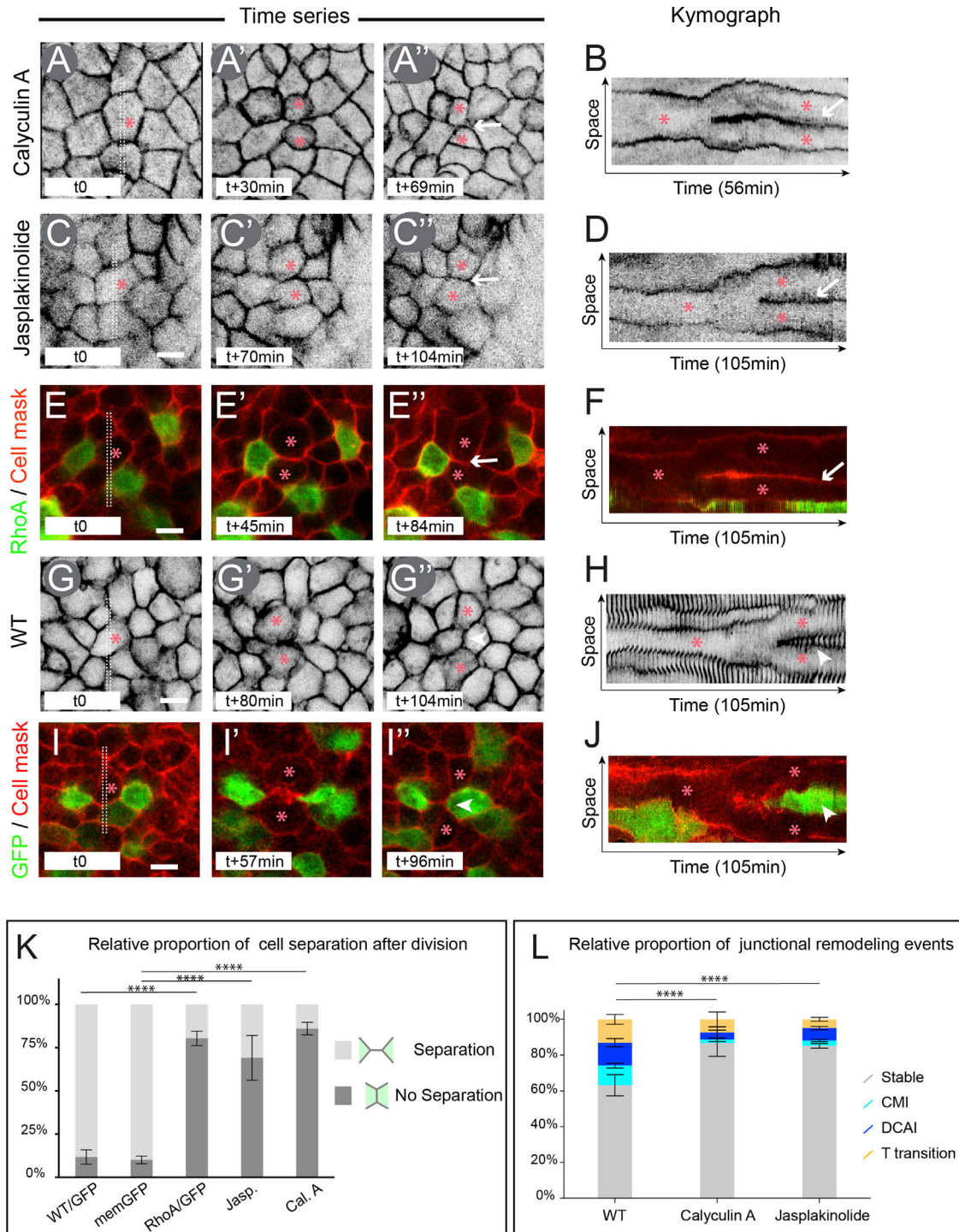
Figure 6. Actin and Myosin Dynamics Control Cell Division-Mediated Intercalation

(A–D) Time series of a memGFP transgenic embryo treated with: the myosin phosphatase inhibitor calyculin A (A) or the F-actin stabilizer jasplakinolide (C) with corresponding kymograph (B and D) of the region boxed in (A) and (C), revealing the relationship between daughter cells at every time point of the movie.

(E and F) Time series of a RhoA/GFP electroporated embryo and incubated with the Cell Mask membrane dye (red) with corresponding kymograph (F) of the region boxed in (E).

(G and H) Time series of memGFP transgenic embryo with corresponding kymograph (H) of the region boxed in (G).

(I and J) Time series of a GFP electroporated embryo and incubated with the Cell Mask membrane dye (red) with corresponding kymograph (J) of the region boxed in (I).

(legend continued on next page)

(Figures 5E–5G and 5I–5K, white arrows; n = 7/9 cells, 3 embryos and 9/13 cells, 3 embryos for jasplakinolide and calyculin A, respectively). Moreover, contact-free cell interfaces, devoid of E-cadherin immunostaining, were observed to be associated with these cortical accumulations of F-actin and pMyosin (Figures 5E–5G and 5I–5K, white asterisks). These results show that increasing myosin and F-actin stability in epithelial cells prevents the dividing cell from bringing distant neighbors into contact, a situation strikingly reminiscent of cell divisions in stage X embryos, when rearrangement of daughter cells does not take place.

We thus decided to observe the effect of increasing actomyosin stability on epithelial cell rearrangements using live imaging microscopy. To this end, we live-imaged embryos incubated with calyculin A or jasplakinolide, which allows uniform perturbation of pMyosin and F-actin turnover within the epithelial embryo (Figures 6A–6D). Notably, at the concentrations we used, neither jasplakinolide nor calyculin A induced a remarkable decrease in cell division (6% decrease for both jasplakinolide and calyculin A compared with control embryos, as counted per number of dividing cells/μm^2 per hour; n = 1,100 cells, 4 embryos and n = 1,111 cells, 3 embryos, respectively). In addition, we electroporated RhoA, which enables stabilization of the actomyosin cytoskeleton in a more selective way due to the mosaic overexpression resulting from the electroporation method (Figures 6E, 6F, and S5J–S5S), therefore allowing us to monitor the behavior of wild-type dividing cells next to RhoA-overexpressing cells (Figures 6E–6E″). In embryos treated with calyculin A and jasplakinolide, and in RhoA-electroporated embryos, separation of daughter cells was greatly affected, with 85% (n = 181, 3 embryos), 69% (n = 129; 3 embryos), and 80% (n = 205, 4 embryos) of daughter cells remaining in contact for at least 30 min after cytokinesis was complete (Figures 6A–6F [white arrows], and 6K; Movie S6), versus 10% in control memGFP transgenic embryos (n = 530, 5 embryos) and 12% in GFP electroporated embryos (n = 239, 6 embryos) (Figures 6G–6K). Moreover, analysis of cell-cell junctions over time revealed that CMI, DCAI, and T processes were largely affected in calyculin A-treated (87% of "stable" junctions, 2% CMI, 4% DCAI, and 7% T processes; n = 385 junctions analyzed, 3 embryos) and jasplakinolide-treated (85% "stable" junctions, 3% CMI, 7% DCAI, and 5% T processes; n = 568 junctions analyzed, 3 embryos) embryos (Figure 6L; see also Figure S7). These results show that calyculin A and jasplakinolide treatments dramatically increase cell-cell junction stability. Strikingly, the behavior of cell-cell junctions under these conditions resembles the behavior of junctions of a stage X embryo, during which epithelial cells exhibit increased actomyosin levels and cell division does not promote cell rearrangements. Altogether, these results show that increasing actomyosin cytoskeleton stability dramatically increases junctional stability over time and prevents dividing cells from remodeling

nearby junctions, consequently impairing cell division-mediated rearrangements.

DISCUSSION

This study has identified that epithelial rearrangements mediated by cell division underlie the spatial patterning of gastrulation movements in chick. As cells divide and dramatically change shape throughout the epithelial embryo, they bring originally distant cells (their immediate neighbors) into contact, thereby promoting intercalation events. The interplay between the actomyosin of dividing cells and the actomyosin of neighboring non-dividing cells prevents rearrangements at stage X before the onset of gastrulation movements, whereas it favors cell division-mediated rearrangements as gastrulation movements take place. Because cells continuously (although asynchronously) divide within the epithelial embryo, cells constantly rearrange, allowing the generation of properly patterned gastrulation movements (Figure 7).

Cell Division as an Epithelial Cell Rearrangement Driver

As mentioned above, a direct role for cell division in promoting epithelial cell rearrangements has not been reported to date in *Drosophila, C. elegans, Danio rerio*, and *Xenopus* models. Indeed it has been implied that the generation of a common cell-cell interface between daughter cells might be a conserved feature among Metazoa (Gibson et al., 2006). Luminal mitosis has been observed to be associated with cell dispersal in the mouse ureteric bud (Packard et al., 2013), and more recently cell division has been observed to be associated with rearrangements during mouse limb ectoderm morphogenesis (Lau et al., 2015), challenging the view that daughter cells do not rearrange upon division. While these studies did not examine the role of cell division in cell-cell intercalation and its effect on epithelial morphogenesis, our findings showing that cell division is required for the generation of gastrulation movements leads us to propose that the formation of new cell-cell contacts following cell division might be a broad regulatory mechanism in epithelium morphogenesis. The observations that cell division appears to be associated with epithelial cell rearrangements in other amniote epithelia is intriguing and shows that special attention should be given to the role of cell division in promoting cell rearrangements, as it is very likely that cell division-mediated intercalations in general might underlie various morphogenetic processes in a number of different epithelial tissues in developmental, homeostatic, or pathological contexts.

Role of Cell Division-Mediated Rearrangements in the Generation of Gastrulation Movements

Previous studies have shown that a combination of cell shape changes, mediolateral intercalation, and ingression events at

(K) Quantification of the proportion of cells exhibiting a daughter-daughter cell junction in all aforementioned conditions. Error bars represent SEM with two-way ANOVA test p value between bars. ****p < 0.0001.

(L) Quantifications of the relative proportion of stable junctions and CMI, DCAI, and T transitions in wild-type (WT), calyculin A-treated, and jasplakinolide-treated embryos. Error bars represent SEM with χ^2 test p value between bars. ****p < 0.0001.

Arrowheads point to a novel junction between initially distant neighbors, arrows point to a daughter-daughter cell junction, and red asterisks indicate a dividing cell and its resulting daughter cells.

Scale bar represents 10 μm. See also Figures S5–S7 and Movie S6.
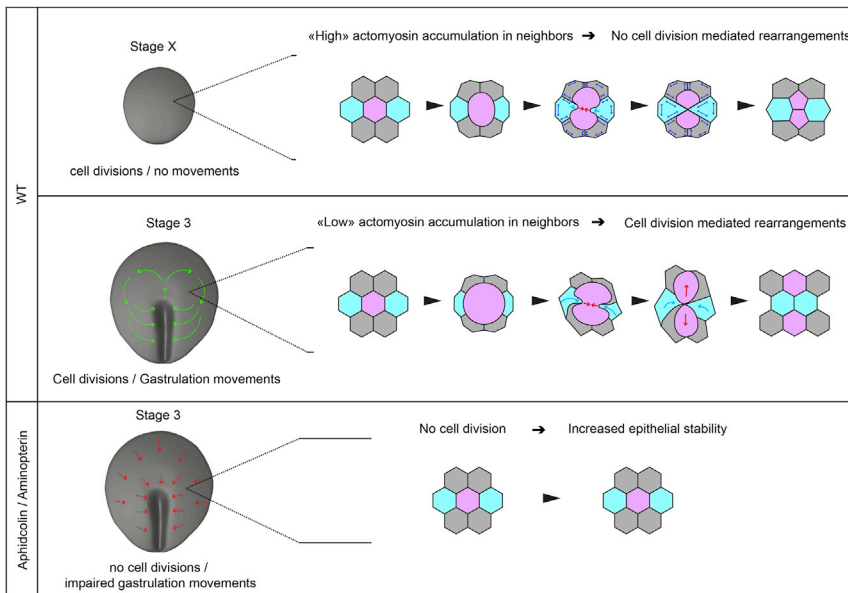
Figure 7. Model for the Role and Control of Cell Division during Gastrulation

Upper: At stage X, before gastrulation movements initiate, epithelial cells divide (red arrows) without promoting rearrangements, epithelial cells exhibit higher actomyosin accumulation: the dividing cell induces very local deformation of neighbors (light blue arrow) as they resist deformation and exhibit high junctional stability (double arrows in blue). These cells consequently fail to move in between daughters and intercalation does not take place. Middle: At stage 3, as gastrulation movements are taking place, cell division promotes epithelial cell rearrangements. Epithelial cells exhibit lower actomyosin accumulation, enabling dividing cells (red arrows) to deform and displace neighbors (light blue arrow), bringing them in between the resulting daughters. Lower: In the absence of cell division, epithelial stability is increased as cell division-mediated rearrangements do not take place. Epithelial cells are likely pulled (red arrows) toward the primitive streak, where intercalation/ingression events take place (Rozbicki et al., 2015; Voiculescu et al., 2007, 2014).

the posterior marginal zone of the early embryo drive primitive streak formation and elongation (Rozbicki et al., 2015; Voiculescu et al., 2007, 2014). Such cell interactions have been proposed to be the driving force of gastrulation movements whereby the rotational movements would ensue as "propagation" of the cell displacements taking place at the site of primitive streak formation. However, whether specific cell behaviors take place in the epithelial embryo to ensure proper patterning of gastrulation movements has remained unaddressed. In the present study, we focused on such specific cellular behaviors. Our data show that cell divisions and associated cell rearrangements are required for the proper spatial patterning of gastrulation movements but that they do not drive the movement itself. When cell division-mediated rearrangements are inhibited (aphidicolin and aminopterin treatments), cell movements can still be observed but the spatial pattern is changed: cells do not display the two symmetrical whorls but instead converge directly toward the primitive streak. An attractive hypothesis is that cell division, through constant cell rearrangements, allows epithelial cells to accommodate (through constant and isotropic stress relaxation) the forces generated by cell-cell interactions taking place at the primitive streak (Rozbicki et al., 2015; Voiculescu et al., 2007, 2014), whereas in the absence of cell division the whole epithelial sheet, being greatly stabilized, appears to be consequently pulled toward the primitive streak "as a whole" by these same forces (Figure 7), although this remains to be experimentally demonstrated. Interestingly, orientation of cell division is not aligned with tissue flow, and UV laser isolation of epithelial regions shows that daughter cell separation appears to be independent of the local directed strains arising from the primitive streak-forming region. Therefore, the effect of cell division on global tissue flow cannot solely be explained by a tension-induced stress-relieving mechanism. It is possible, however, that cell division by promoting constant rearrangements might act by modulating the mechanical properties of the epithelial tissue (e.g. fluidization of the tissue). In the future, it will be partic-

ularly interesting to test whether a combination of changes in mechanical properties of the epiblast and local directed strains induced by the primitive streak-forming region could explain large-scale tissue movements observed during gastrulation.

Molecular Mechanisms Underlying Cell Division-Mediated Rearrangements

We also investigated how cell division-mediated intercalations are controlled at the molecular level. We find, similar to what has been described in several *Drosophila* epithelia, that cell division in the early chick epiblast can be regarded as a multicellular process whereby immediate neighbors at stage X play a role in the formation of daughter-daughter cell junctions; however, as gastrulation movements take place in chick, cell division leads to an opposite outcome (i.e. cell intercalation, Figure 7). We identified two specific behaviors: intercalation of neighboring cells between daughter cells (CMI) and intercalation of daughter cells between neighbors (DCAI), which consequently lead to dramatic rearrangements in the vicinity of a dividing cell. Interestingly, although CMI implies the addition of a novel junction through cytokinesis, it is somehow similar to T1 and rosette processes described in *Drosophila* (Bertet et al., 2004; Blankenship et al., 2006), as a myosin-based contraction (cytokinetic ring in CMI and planar junction shortening in T1/rosette processes) brings into contact originally distant cells. However, we show that in chick, intercalation initiates basally, expands apically, and eventually occurs in the plane of the epithelium. It has been shown in other systems that cadherin engagement triggers contact stabilization and expansion through activation of the Rac1 and Arp2/3 complex (Betson et al., 2002; Nakagawa et al., 2001; Noren et al., 2001; Perez et al., 2008; Verma et al., 2004; Yamada and Nelson, 2007; Yamazaki et al., 2007). These data, together with our results, are in support of basal engagement of E-cadherin between originally distant neighbors as a critical step in the formation of a stable novel junction, and thereby in cell intercalation events. In turn, the mechanisms underlying DCAI are less clear,

as no specific myosin enrichments could be observed in neighbors (data not shown) that could explain active intercalation of daughter cells, as observed in T1 processes in *Drosophila*. It is possible that DCAI might be a passive consequence of cell division, in a local environment that is permissive to rearrangements or in an active process whereby daughter cells transiently acquire an "intra-epithelial" motility.

At the molecular level, comparison between stage X and stage 3 embryos indicated the actomyosin cytoskeleton in non-dividing cells as a regulator of these behaviors. Strikingly, in stage X embryos when cell division does not drive rearrangements, actin and myosin accumulate basolaterally in immediate neighbors of a dividing cell, formation of a novel contact (between distant neighbors) does not take place, and adhesion disengagement between the dividing cells and its neighbors can even be observed. A similar phenomenon has been observed in the *Drosophila* embryo and pupal notum during the formation of the daughter-daughter cell interface (Founounou et al., 2013; Guillot and Lecuit, 2013b; Herszterg et al., 2013), although in chick actomyosin accumulation and adhesion disengagement occur along the basolateral interface. From our analysis, the major difference between the embryonic and pupal notum epithelia in *Drosophila* and the early chick embryonic epithelium is that E-cadherin can be found basolaterally in chick epithelial cells. It is thus possible that since myosin and actin do not accumulate basolaterally in epithelial cells of stage 3 embryos, as a dividing cell rounds up, contracts, and splits, it can freely deform and displace its immediate and adherent neighbors, bringing them into contact without resistance. We finally demonstrate the functional relevance of actin and myosin in this process by increasing cortical actomyosin accumulation uniformly in the epiblast using jasplakinolide and calyculin A, or specifically in neighboring cells using RhoA. Such accumulation of actomyosin at the cortex impairs the formation of novel contacts basally and subsequent cell division-mediated rearrangements normally taking place at stage 3, recapitulating situations and behaviors observed at stage X. Taken together, our results provide a mechanistic framework for understanding how cell division can lead to different remodeling outcomes within an epithelial tissue, and how it affects its morphogenesis on the mesoscopic scale.

EXPERIMENTAL PROCEDURES

Embryo Culture, Imaging, and Laser Dissection
Fertilized chicken eggs were ordered from a commercial source (EARL Morizeau) and memGFP transgenic chicken eggs were generously provided by Dr. Feifei Song, Dr. Adrian Sherman, and Dr. Helen Sang from the Roslin Institute. Eggs were collected at stage X and cultured using a modified version of the EC culture system (Chapman et al., 2001) until stage 3+ and transferred into glass-bottom Petri dishes (Mattek) with semisolid albumin/agarose (0.2%) for imaging, with or without drugs: aphidicolin (30–50 μm), aminopterin (100 μm), jasplakinolide (10 μm) and calyculin A (0.1 μM). Embryos were then imaged at 38°C using an inverted confocal microscope (Zeiss LSM 700 and LSM 880) or a two-photon microscope (Zeiss, NLO LSM 7MP) coupled to a Chameleon Ti/Saph laser (Coherent) at 840 nm wavelength using 10×, 40×, or 63× long-distance objectives. The tiling/stitching feature of the Zen software (Zeiss) was used to acquire large embryonic regions (about 1 mm²/5,000–10,000 cells) with a 40× objective. Laser microdissections were performed using a 355-nm pulsed laser (35%–50% power), a UGA-42 module from Rapp Optoelectronic coupled to a Zeiss LSM 880 and a 10× objective.

Image Analysis and Quantification
Images were analyzed using ImageJ and Imaris (Bitplane) software. All quantifications were performed manually on registered movies (Thévenaz et al., 1998) by visual inspection, following cells or junctions across time. For all experiments, daughter cells were scored as separated when they did not share a common interface 30 min after the completion of cytokinesis. Quantifications of daughter cell separation at stage X were performed during the first 3 hr of development and within 3 hr after exposure to the drugs in stage 3 embryos. For cell-cell junction analysis, 1-hr-long movies were analyzed; regions were randomly chosen but the number of cell divisions per total number of junctions analyzed within these regions was kept constant, except for aphidicolin- and aminopterin-treated embryos in which cell division was largely inhibited. Junctions were classified into four different states, based on whether the cell-cell junction exhibited neighbor exchange: Stable: pair of neighbors remained unchanged; T transition: T1 or T2 process (i.e. cell division-independent neighbor exchange); CMI transition: dividing cell-neighbor junction involved in an intercalation event between daughter cells; DCAI transition: T1 process involving a daughter cell (see Movie S3). The rate of cell division in drug-treated embryos was measured by counting the number of dividing cells per mm² per hour, normalized to stage 3 embryo rates.

FRAP Experiments
For FRAP experiments, embryos were electroporated with GFP-Myosin at stage X and then incubated for 5 hr until a clear cortical GFP-Myosin signal could be visualized. For stage 3, the same embryos for which FRAP was performed at stage X were kept incubated overnight for a total incubation time of 14 hr. The GFP-Myosin signal did not show any significant difference in intensity between both stages, and identical photobleaching and imaging conditions were used. A 10 × 10-pixel cortical region was photobleached using a 488-nm laser at 100% (pixel dwell time of 100 μs for ten iterations). Cells were then imaged every 1.5 s for at least 250 s using a Zeiss LSM 700 confocal and a 40× objective. All quantifications were performed in Fiji. Images were adjusted for xy drift with the plugin: "Linear Stack Alignment with SIFT" using a translational transformation. ROIs within the bleached and non-bleached areas were then manually selected to compensate for acquisition bleach and normalize the values. The curve fitting of the data was done using a custom-made plugin in MATLAB (MathWorks). Final plots were done using Prism (GraphPad Software).

Chick Embryo Electroporation and Immunofluorescence
Embryos were electroporated with RhoA/GFP (a kind gift from Gojun Sheng) or GFP only, in custom-made electroporation chambers using a NEPA21 (Sonidel) electroporator with two poring pulses of 15 V, 5 ms delay, and three transfer pulses of 10 V, 50 ms delay. Electroporated embryos were incubated with Cell Mask Deep Red (Invitrogen) prior to live imaging experiments. In brief, 0.5 μl of Cell Mask Deep Red stock solution (5 mg/ml in DMSO) was diluted in 250 μl of Hank's balanced salt solution; 50 μl of this dilution was then deposited on the ventral side of the embryo and incubated for 15 min prior to imaging. For antibody stainings, embryos were incubated with Phalloidin-Alexa 488 (1:100; Molecular Probes), antibodies against E-cadherin (1:500, BD Science), pMyosinII (1:50; Cell Signaling), and Hoechst (1:1000, Molecular Probes) overnight, washed for 24 hr, incubated overnight with Alexa-coupled secondary antibodies, and washed for 24 hr. All incubation and washes were performed in PBS/BSA 0.2%, Triton 0.1%/SDS 0.02%. Embryos were then mounted between slides, coverslipped, and imaged using a Zeiss LSM 700 or LSM 880.

SUPPLEMENTAL INFORMATION

Supplemental Information includes seven figures and six movies and can be found with this article online at http://dx.doi.org/10.1016/j.devcel.2016.01.007.

AUTHOR CONTRIBUTIONS

REFERENCES

Baena-López, L.A., Baonza, A., and García-Bellido, A. (2005). The orientation of cell divisions determines the shape of *Drosophila* organs. Curr. Biol. *15*, 1640–1644.

Bertet, C., Sulak, L., and Lecuit, T. (2004). Myosin-dependent junction remodelling controls planar cell intercalation and axis elongation. Nature *429*, 667–671.

Betson, M., Lozano, E., Zhang, J., and Braga, V.M.M. (2002). Rac activation upon cell-cell contact formation is dependent on signaling from the epidermal growth factor receptor. J. Biol. Chem. *277*, 36962–36969.

Bischoff, M., and Cseresnyés, Z. (2009). Cell rearrangements, cell divisions and cell death in a migrating epithelial sheet in the abdomen of *Drosophila*. Development *136*, 2403–2411.

Blankenship, J.T., Backovic, S.T., Sanny, J.S.P., Weitz, O., and Zallen, J.A. (2006). Multicellular rosette formation links planar cell polarity to tissue morphogenesis. Dev. Cell *11*, 459–470.

Bubb, M.R., Senderowicz, A.M., Sausville, E.A., Duncan, K.L., and Korn, E.D. (1994). Jasplakinolide, a cytotoxic natural product, induces actin polymerization and competitively inhibits the binding of phalloidin to F-actin. J. Biol. Chem. *269*, 14869–14871.

Campinho, P., Behrndt, M., Ranft, J., Risler, T., Minc, N., and Heisenberg, C.-P. (2013). Tension-oriented cell divisions limit anisotropic tissue tension in epithelial spreading during zebrafish epiboly. Nat. Cell Biol. *15*, 1405–1414.

Cavey, M., and Lecuit, T. (2009). Molecular bases of cell-cell junctions stability and dynamics. Cold Spring Harb Perspect. Biol. *1*, a002998.

Cavey, M., Rauzi, M., Lenne, P.-F., and Lecuit, T. (2008). A two-tiered mechanism for stabilization and immobilization of E-cadherin. Nature *453*, 751–756.

Chapman, S.C., Collignon, J., Schoenwolf, G.C., and Lumsden, A. (2001). Improved method for chick whole-embryo culture using a filter paper carrier. Dev. Dyn. *220*, 284–289.

Cui, C., Yang, X., Chuai, M., Glazier, J.A., and Weijer, C.J. (2005). Analysis of tissue flow patterns during primitive streak formation in the chick embryo. Dev. Biol. *284*, 37–47.

Engl, W., Arasi, B., Yap, L.L., Thiery, J.P., and Viasnoff, V. (2014). Actin dynamics modulate mechanosensitive immobilization of E-cadherin at adherens junctions. Nat. Cell Biol. *16*, 587–594.

Founounou, N., Loyer, N., and Le Borgne, R. (2013). Septins regulate the contractility of the actomyosin ring to enable adherens junction remodeling during cytokinesis of epithelial cells. Dev. Cell *24*, 242–255.

Gibson, M.C., Patel, A.B., Nagpal, R., and Perrimon, N. (2006). The emergence of geometric order in proliferating metazoan epithelia. Nature *442*, 1038–1041.

Gong, Y., Mo, C., and Fraser, S.E. (2004). Planar cell polarity signalling controls cell division orientation during zebrafish gastrulation. Nature *430*, 689–693.

Gräper, L. (1929). Die Primitiventwicklung des Hühnchens nach stereokinematographischen Untersuchungen, kontrolliert durch vitale Farbmarkierung und verglichen mit der Entwicklung anderer Wirbeltiere. Dev. Genes Evol. *116*, 382–429.

Guillot, C., and Lecuit, T. (2013a). Mechanics of epithelial tissue homeostasis and morphogenesis. Science *340*, 1185–1189.

Guillot, C., and Lecuit, T. (2013b). Adhesion disengagement uncouples intrinsic and extrinsic forces to drive cytokinesis in epithelial tissues. Dev. Cell *24*, 227–241.

Harrell, J.R., and Goldstein, B. (2011). Internalization of multiple cells during *C. elegans* gastrulation depends on common cytoskeletal mechanisms but different cell polarity and cell fate regulators. Dev. Biol. *350*, 1–12.

Herszterg, S., Leibfried, A., Bosveld, F., Martin, C., and Bellaiche, Y. (2013). Interplay between the dividing cell and its neighbors regulates adherens junction formation during cytokinesis in epithelial tissue. Dev. Cell *24*, 256–270.

Ishihara, H., Martin, B.L., Brautigan, D.L., Karaki, H., Ozaki, H., Kato, Y., Fusetani, N., Watabe, S., Hashimoto, K., and Uemura, D. (1989). Calyculin A and okadaic acid: inhibitors of protein phosphatase activity. Biochem. Biophys. Res. Commun. *159*, 871–877.

Kieserman, E.K., Glotzer, M., and Wallingford, J.B. (2008). Developmental regulation of central spindle assembly and cytokinesis during vertebrate embryogenesis. Curr. Biol. *18*, 116–123.

Knox, A.L., and Brown, N.H. (2002). Rap1 GTPase regulation of adherens junction positioning and cell adhesion. Science *295*, 1285–1288.

Lau, K., Tao, H., Liu, H., Wen, J., Sturgeon, K., Sorfazlian, N., Lazic, S., Burrows, J.T.A., Wong, M.D., Li, D., et al. (2015). Anisotropic stress orients remodelling of mammalian limb bud ectoderm. Nat. Cell Biol. *17*, 569–579.

LeGoff, L., Rouault, H., and Lecuit, T. (2013). A global pattern of mechanical stress polarizes cell divisions and cell shape in the growing *Drosophila* wing disc. Development *140*, 4051–4059.

Mao, Y., Tournier, A.L., Hoppe, A., Kester, L., Thompson, B.J., and Tapon, N. (2013). Differential proliferation rates generate patterns of mechanical tension that orient tissue growth. EMBO J. *32*, 2790–2803.

Marinari, E., Mehonic, A., Curran, S., Gale, J., Duke, T., and Baum, B. (2012). Live-cell delamination counterbalances epithelial growth to limit tissue overcrowding. Nature *484*, 542–545.

Morin, X., and Bellaïche, Y. (2011). Mitotic spindle orientation in asymmetric and symmetric cell divisions during animal development. Dev. Cell *21*, 102–119.

Nakagawa, M., Fukata, M., Yamaga, M., Itoh, N., and Kaibuchi, K. (2001). Recruitment and activation of Rac1 by the formation of E-cadherin-mediated cell-cell adhesion sites. J. Cell Sci. *114*, 1829–1838.

Noren, N.K., Niessen, C.M., Gumbiner, B.M., and Burridge, K. (2001). Cadherin engagement regulates Rho family GTPases. J. Biol. Chem. *276*, 33305–33308.

Olivier, N., Luengo-Oroz, M.A., Duloquin, L., Faure, E., Savy, T., Veilleux, I., Solinas, X., Débarre, D., Bourgine, P., Santos, A., et al. (2010). Cell lineage reconstruction of early zebrafish embryos using label-free nonlinear microscopy. Science *329*, 967–971.

Packard, A., Georgas, K., Michos, O., Riccio, P., Cebrian, C., Combes, A.N., Ju, A., Ferrer-Vaquer, A., Hadjantonakis, A.-K., Zong, H., et al. (2013). Luminal mitosis drives epithelial cell dispersal within the branching ureteric bud. Dev. Cell *27*, 319–330.

Perez, T.D., Tamada, M., Sheetz, M.P., and Nelson, W.J. (2008). Immediate-early signaling induced by E-cadherin engagement and adhesion. J. Biol. Chem. *283*, 5014–5022.

Rozbicki, E., Chuai, M., Karjalainen, A.I., Song, F., Sang, H.M., Martin, R., Knölker, H.-J., MacDonald, M.P., and Weijer, C.J. (2015). Myosin-II-mediated cell shape changes and cell intercalation contribute to primitive streak formation. Nat. Cell Biol. *17*, 397–408.

Saburi, S., Hester, I., Fischer, E., Pontoglio, M., Eremina, V., Gessler, M., Quaggin, S.E., Harrison, R., Mount, R., and McNeill, H. (2008). Loss of Fat4 disrupts PCP signaling and oriented cell division and leads to cystic kidney disease. Nat. Genet. *40*, 1010–1015.

Sheikh, S., Gratzer, W.B., Pinder, J.C., and Nash, G.B. (1997). Actin polymerisation regulates integrin-mediated adhesion as well as rigidity of neutrophils. Biochem. Biophys. Res. Commun. *238*, 910–915.

Thévenaz, P., Ruttimann, U.E., and Unser, M. (1998). A pyramid approach to subpixel registration based on intensity. IEEE Trans. Image Process. *7*, 27–41.

Verma, S., Shewan, A.M., Scott, J.A., Helwani, F.M., den Elzen, N.R., Miki, H., Takenawa, T., and Yap, A.S. (2004). Arp2/3 activity is necessary for efficient formation of E-cadherin adhesive contacts. J. Biol. Chem. *279*, 34062–34070.

Voiculescu, O., Bertocchini, F., Wolpert, L., Keller, R.E., and Stern, C.D. (2007). The amniote primitive streak is defined by epithelial cell intercalation before gastrulation. Nature *449*, 1049–1052.

Voiculescu, O., Bodenstein, L., Lau, I.-J., and Stern, C.D. (2014). Local cell interactions and self-amplifying individual cell ingression drive amniote gastrulation. Elife *3*, e01817.

Wetzel, R. (1929). Untersuchungen am Hühnchen. Die Entwicklung des Keims während der ersten beiden Bruttage. Wilhelm Roux Arch. Entwickl. Mech. Org. *119*, 188–321.

Wu, S.K., Gomez, G.A., Michael, M., Verma, S., Cox, H.L., Lefevre, J.G., Parton, R.G., Hamilton, N.A., Neufeld, Z., and Yap, A.S. (2014). Cortical F-actin stabilization generates apical-lateral patterns of junctional contractility that integrate cells into epithelia. Nat. Cell Biol. *16*, 167–178.

Wyatt, T.P.J., Harris, A.R., Lam, M., Cheng, Q., Bellis, J., Dimitracopoulos, A., Kabla, A.J., Charras, G.T., and Baum, B. (2015). Emergence of homeostatic epithelial packing and stress dissipation through divisions oriented along the long cell axis. Proc. Natl. Acad. Sci. USA *112*, 5726–5731.

Yamada, S., and Nelson, W.J. (2007). Localized zones of Rho and Rac activities drive initiation and expansion of epithelial cell-cell adhesion. J. Cell Biol. *178*, 517–527.

Yamazaki, D., Oikawa, T., and Takenawa, T. (2007). Rac-WAVE-mediated actin reorganization is required for organization and maintenance of cell-cell adhesion. J. Cell Sci. *120*, 86–100.